Environmental Science & Technology

ARTICLE

pubs.acs.org/est

Hydrophobic Interactions Increase Attachment of Gum Arabic- and PVP-Coated Ag Nanoparticles to Hydrophobic Surfaces

Jee Eun Song,[†] Tanapon Phenrat,[†,#] Stella Marinakos,[∥] Yao Xiao,[⊥] Jie Liu,[∥] Mark R. Wiesner,[⊥] Robert D. Tilton,[‡,§] and Gregory V. Lowry*[,†]

[†]Center for Environmental Implications of Nanotechnology (CEINT) and Department of Civil & Environmental Engineering, [‡]Department of Chemical Engineering, and [§]Department of Biomedical Engineering, Carnegie Mellon University, Pittsburgh, Pennsylvania 15213, United States

[#]Department of Civil Engineering, Naresuan University, Phitsanulok, Thailand

[∥]Department of Chemistry and [⊥]Department of Civil and Environmental Engineering, Duke University, Durham, North Carolina 27708, United States

Supporting Information

ABSTRACT: A fundamental understanding of attachment of surface-coated nanoparticles (NPs) is essential to predict the distribution and potential risks of NPs in the environment. Column deposition studies were used to examine the effect of surface-coating hydrophobicity on NP attachment to collector surfaces in mixtures with varying ratios of octadecylichlorosilane (OTS)-coated (hydrophobic) glass beads and clean silica (hydrophilic) glass beads. Silver nanoparticles (AgNPs) coated with organic coatings of varying hydrophobicity, including citrate, polyvinylpyrrolidone (PVP), and gum arabic (GA), were used. The attachment efficiencies of GA and PVP AgNPs increased by 2- and 4-fold, respectively, for OTS-coated glass beads compared to clean glass beads. Citrate AgNPs showed no substantial change in attachment efficiency for hydrophobic compared to hydrophilic surfaces. The attachment efficiency of PVP-, GA-, and citrate-coated AgNPs to hydrophobic collector surfaces correlated with the relative hydrophobicity of the coatings. The differences in the observed attachment efficiencies among AgNPs could not be explained by classical DLVO, suggesting that hydrophobic interactions between AgNPs and OTS-coated glass beads were responsible for the increase in attachment of surface-coated AgNPs with greater hydrophobicity. This study indicates that the overall attachment efficiency of AgNPs will be influenced by the hydrophobicity of the NP coating and the fraction of hydrophobic surfaces in the environment.

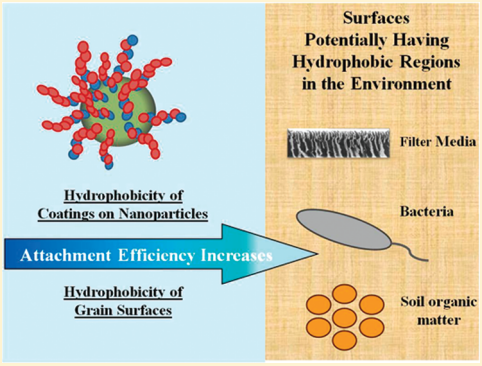

INTRODUCTION

Transport of particles in porous media including colloids,[1] bacteria,[2,3] and virus[4] have been studied extensively. These studies have provided a fundamental understanding of the physicochemical interactions between particles and collectors, including van der Waals attraction, electrostatic repulsion, and acid−base interactions. They have also demonstrated the potential for hydrophobic interactions between particles and collectors.[5−7] Recently, the transport of engineered nanoparticles (ENPs) in porous media has received a great deal of attention[8] because it determines the distribution of ENPs in environmental media and potential for exposure,[9] which are essential components of risk assessment of ENPs.

ENPs released into the environment are typically coated with natural or engineered organic materials, which are known to considerably influence the attachment of ENPs.[10−12] Particularly, polymeric organic coatings on ENPs cause steric interactions derived from osmotic pressure due to overlapping of polymer segments and elastic repulsions due to deformation of attached polymeric chains. The range and magnitude of the steric interactions can be modeled if several characteristics of the organic coatings are known, including molecular weight, surface concentration, layer thickness, and electrokinetic potential.[13] Extended DLVO theory (XDLVO), which extends DLVO theory by the inclusion of steric interactions, has been used to explain the effect of steric interactions on transport of ENPs in porous media.[14]

In addition to steric interactions, polymeric coatings on ENP surfaces may also lead to hydrophobic interactions between particles and collectors because polymeric coatings are often amphiphilic, i.e., having both hydrophobic and hydrophilic properties. Hydrophobic interactions have been broadly used to explain a variety of natural phenomena, including separation of oil/water mixtures, protein folding, and the aggregation and self-assembly of hydrophobic entities.[15] In bacteria and virus transport studies, particle surface hydrophobicity has been shown to be an important factor for their attachment, for both hydrophilic and

Received: February 16, 2011
Accepted: May 27, 2011
Revised: May 24, 2011
Published: June 21, 2011

hydrophobic collectors.[3,7] However, the effect of hydrophobicity of the surface coatings on ENPs on their attachment to hydrophilic and hydrophobic surfaces has not been reported.

The goal of this study is to investigate the effects of hydrophobic organic coatings on ENP attachment, particularly when the collector surfaces are chemically heterogeneous, i.e., having both hydrophilic and hydrophobic surfaces. Attachments of silver nanoparticles (AgNPs) of similar size but with three coatings of differing hydrophobicity—citrate (anionic), gum arabic (GA, a complex polysaccharide/glycoprotein mixture, negatively charged at neutral pH), and polyvinylpyrrolidone (PVP, nonionic)—were measured in columns packed with the mixture of clean (hydrophilic) and octadecylichlorosilane (OTS)-coated (hydrophobic) glass beads. The study indicates that NP coatings with higher hydrophobicity have greater attachment to hydrophobic surfaces. This attractive interaction is not predicted from XDLVO theory that accounts for electrosteric repulsions afforded by the coatings but ignores hydrophobic interactions.

MATERIALS AND METHODS

Preparation of Surface Modified AgNPs. Three types of surface-coated AgNPs were synthesized by reduction of silver nitrate in the presence of citrate, GA, and PVP, respectively. The detailed synthesis procedure is provided in the Supporting Information (SI). Approximately 100 ppm of each coated AgNP in 1 mM $NaHCO_3$ solution was washed before use to remove excess polymer in dispersion. Particles were ultracentrifuged (Sorvall Ultracentrifuge OTD65B) at 58 800*g* for 1 h to separate the particles from the dispersion. The supernatant was decanted, and then the particles were resuspended in 1 mM $NaHCO_3$. This process was conducted twice before samples were used.

Preparation of Hydrophobic Porous Media. Soda lime glass beads (Potters Industries Inc., Malvern, PA) with a median diameter of 0.35 mm were thoroughly washed by rinsing with hexane, methanol, hydrochloric acid, and DI water to remove impurities. To produce hydrophobic glass beads, they were coated with uncharged octadecylichlorosilane (OTS) (M_w = 388, Sigma) following the procedure of Kumar et al.:[16] 50 g of washed glass beads were immersed in a 2 mM OTS solution in hexadecane−chloroform (90:10 by volume) and rotated on an end-over-end rotator at 30 rpm for 30 min. The excess OTS was removed from the glass bead surfaces by rinsing with chloroform. OTS-covered glass beads were rinsed again with methanol, 1 M HCl, and DI water sequentially until the rinsewater reached neutral pH. The glass beads were then dried at 110 °C for 24 h.

Characterization of AgNPs. Particle size distributions were measured by dynamic light scattering (DLS) (Malvern Zetasizer, Southborough, MA) and transition electron microscopy (TEM) (Philips, Eindhoven, Netherlands). The DLS size measurements were conducted in triplicate using backscatter (173°) detection on samples containing 50 mg/L AgNPs after 10 min of sonication (550 Sonic Dismembrator, Fisher Scientific). Intensity-weighted hydrodynamic particle size distributions were calculated from the intensity-autocorrelation functions using the CONTIN algorithm, assuming the Stokes−Einstein equation for spherical particles. The intensity size distributions were converted to volume-weighted size distributions using the refractive index of 0.135 for silver[17] (Figure S1 in SI). The TEM sizes of at least 100 particles were measured for each of three AgNPs with a Philips 301 TEM operated at 80 kV (Figure S2 in SI).

We performed electrophoretic mobility (EPM) measurements for bare AgNPs (Nanoamor, Houston, TX) as well as citrate-, GA-, and PVP-coated AgNPs in 30 mg/L using a Malvern Zetasizer (Figure S3 in SI). The samples were ultrasonicated for 5 min before each EPM measurement. Duplicate measurements were made in $NaNO_3$ solutions with concentration ranging from 5 to 80 mM at pH 8.1 ± 0.1. Smoluchowski's model was used to estimate the ζ-potential for uncoated and citrate AgNPs. Ohshima's soft particle theory[18] was used to estimate the layer thickness and surface potential of the adsorbed polymer layer. The details for the method used to estimate adsorbed polymer layer thickness and surface potential are described in the SI.

Thermal gravity analysis (TGA) (SDT Q600, TA Instruments, New Castle, DE) was used to measure the surface concentrations of organic coatings (citrate, GA, and PVP) on AgNPs. For sample preparation, the surface-coated AgNPs as well as bare AgNPs were washed using an ultracentrifuge as described above and freeze-dried at 23 °C to a dry powder. Approximately 5−10 mg of each sample was used: bare AgNPs, surface-modified AgNPs (citrate-, GA-, and PVP-coated AgNPs), and organic coatings alone (citrate, GA, and PVP). A heat ramp of 5 °C/min up to 700 °C in air was set up to measure the weight change before and after heating. Details of the TGA results are provided in Figure S4 and Table S1 in the SI.

Characterization of Collector Surfaces. The relative hydrophobicity of clean and OTS-coated collector surfaces was examined by the modified sessile drop method introduced by Bachmann et al.[19] A smooth and flat plastic slide was covered with double-sided adhesive tape (3M, St. Paul, MN). Dry glass beads were attached to the tape by pressing with a 100 g weight for 5 s. The board was then shaken carefully to remove surplus glass beads. A water droplet with 5 μm diameter was pipetted onto the monolayer of glass beads on the tape. Contact angles were measured 10 times for each sample at 23 °C using a goniometer (Rame-Hart, Netcong, NJ) (Figure S5 in the SI).

The streaming potentials for the clean and OTS-coated glass beads were measured in 20 mM $NaNO_3$ with 1 mM $NaHCO_3$ solution at pH 8.1 using an electrokinetic analyzer (SurPass, Anton Paar, Ashland, VA). A cylindrical cell (1.3 cm diameter by 1 cm length) was filled with either clean glass beads or OTS-coated glass beads. The cell was immersed in an ultrasonic bath for 3 min to obtain a uniform packing density. The streaming potential was converted to ζ-potentials using the Fairbrother−Mastin approach.

Column Deposition Experiments. Deposition experiments were performed in glass columns (C 10/10, GE Healthcare, Waukesha, WI) with a diameter of 1 cm and a length of 10 cm. Columns were packed with approximately 15 g of mixtures of clean and OTS-coated glass beads in an ultrasonic bath (Branson 5200, Danbury, CT) to ensure consistent packing density and column effective porosity. The average porosity of the packed column was determined gravimetrically to be 0.36. An indifferent electrolyte ($NaNO_3$) at an ionic strength of 20 mM and pH 8.1 was used, as this provided breakthrough values of at least 10% but less than 90% for each particle type using the column length and solution conditions described above. A pore water velocity of 0.02 cm/s was used to provide negligible longitudinal dispersion of particles in the column, which is a specified constraint of the attachment efficiency equation. Ten pore volumes of 20 mM $NaNO_3$ plus 1 mM of $NaHCO_3$ solution (pH = 8.1) were flushed through the packed column to eliminate background turbidity

Table 1. Properties of Coatings and AgNPs

	coating molecular weight (g/mol)	DLS intensity size (nm)	DLS volume size (nm)	TEM size (nm)	surface concentration[a] (mg/m^2)	layer thickness[b] (nm)	electrokinetic potential[c] (mV)
citrate AgNPs	294	77 ± 9	9.3 ± 5	10.8 ± 10	0.4−1.3	negligible	−46 ± 0.9
GA AgNPs	250 000	70 ± 6	5.0 ± 4	5.5 ± 2	5.6−17	17 ± 4	−4.7 ± 1
PVP AgNPs	10 000	73 ± 6	9.6 ± 4	7.9 ± 4	2.8−8.4	2.6 ± 1	−14 ± 9

[a] Computed from TGA results (Figure S4 in the SI). [b] Estimated from electrophoretic mobility measurements using Ohshima's model (Figure S3 in the SI). [c] Electrokinetic potentials indicate the ζ-potential of citrate AgNPs and the surface potentials of PVP and GA AgNPs. These potentials were calculated using Smoluchowski's model for citrate AgNPs and Ohshima's model for PVP and GA AgNPs (Figure S9 in the SI).

before AgNPs injection; 50 ppm of AgNP dispersions in 1 mM of $NaHCO_3$ was ultrasonicated for 5 min to break agglomerates formed during storage and then injected into the column in an up-flow configuration. Three pore volumes of nanoparticles were injected by a peristaltic pump. After particle injection, the column was flushed by three additional pore volumes of the ionic solution to obtain a particle breakthrough curve. Effluent samples were collected every 2 min. Influent and effluent AgNP concentrations were analyzed by UV−vis spectroscopy (Varian, Palo Alto, CA) at 405 nm. Deposition experiments for three surface-coated AgNPs were performed at 23 °C in duplicate. In a second series of deposition experiments, OTS-coated glass beads were first flushed with 3 pore volume of 1 mM sodium dodecyl sulfate (SDS) (Fisher) plus the ionic solution prior to AgNP injection to mask the surface hydrophobicity of the OTS-coated glass beads. Prior to introducing AgNPs, the column was flushed with one pore volume of the background electrolyte to remove any desorbed SDS. The electrolyte solution pH was adjusted by 1 mM of NaOH and HNO_3 solution as needed.

Determination of Attachment Efficiency. The deposition of particles in a porous media was quantified in terms of experimental attachment efficiency, α_{exp}:[1,20]

$$\alpha_{exp} = -\ln\left(\frac{C}{C_0}\right)\frac{4a_c}{3(1-\varepsilon)\eta_0 L} \quad (1)$$

where a_c is the radius of glass beads, ε is the packed bed porosity, η_0 is the predicted single-collector contact efficiency in the absence of repulsive interaction, L is the length of the column, and C_0 and C are the influent and effluent particle concentrations, respectively. The normalized column effluent concentration (C/C_0) was obtained from particle breakthrough curves generated by column experiments (Figure S6 in the SI). Within the context of a convective-diffusion system, η_0 is given as

$$\eta_0 = 2.4A_s^{1/3}N_R^{-0.081}N_{Pe}^{-0.715}N_{vdw}^{0.052} + 0.55A_sN_R^{1.675}N_A^{0.125} + 0.22N_R^{-0.24}N_G^{1.11}N_{vdw}^{0.053} \quad (2)$$

where A_s is a porosity-dependent parameter, N_R is the aspect ratio, N_{Pe} is the Peclet number, N_{vdW} is the van der Waals number, N_A is the attraction number, and N_G is the gravity number.[20]

Hydrophobicity of AgNPs and Organic Coatings. To measure the relative hydrophobicity of the organic coatings alone, precipitation experiments were performed by adding ammonium sulfate to sodium citrate, GA, and PVP following Andrews et al.[21] Briefly, sodium citrate, GA, or PVP was added to 50 mL of sodium phosphate buffer (0.05 M, pH 8), as specified in the method used for determining the relative hydrophobicity of macromolecules and proteins.[22] Solid ammonium sulfate was added into the polymer or citrate solutions until the material precipitated (i.e., the cloud point). The solution was then equilibrated on an end-over-end rotator for 5 days at 23 °C. After reaching equilibrium, the turbidity of solutions was measured using a turbidimeter (HACH, Loveland, CO) to determine where precipitation begins. Earlier onset of precipitation indicates greater hydrophobicity of the coating materials.

The surface hydrophobicity of citrate-, GA-, and PVP-coated AgNPs was also measured by adsorption of the hydrophobic dye Rose Bengal (Alfa Aesar, Ward Hill, MA) following Muller et al.;[23] 18 mg/L of Rose Bengal was added to AgNP dispersions with different concentrations covering the range from 5 to 150 mg/L. After 3 h incubation in 0.1 M phosphate buffer, NPs were separated from the supernatant by centrifugation at 185 000g, and the mass of free Rose Bengal in the supernatant was measured by UV−vis spectroscopy at λ = 542.7 nm. The ratio of adsorbed mass of Rose Bengal on NP surfaces vs that in solution was plotted as a function of particle concentration.

RESULTS AND DISCUSSION

Characterization of AgNPs. The measured properties of the three coated AgNPs are provided in Table 1. The intensity-weighted hydrodynamic sizes measured by DLS (DLS intensity sizes) for citrate-, GA-, and PVP-coated AgNPs ranged from 70 to 77 nm. The volume-weighted DLS sizes (DLS volume sizes) ranged from 5.0 to 9.6 nm, consistent with the primary particle sizes observed by TEM (TEM sizes) of 5.5−10.8 nm. This difference between the DLS intensity-weighted and volume-weighted sizes is a result of the weighting in the algorithm used to calculate size; particles are weighted to the sixth power of the particle radius for intensity-weighted size according to Rayleigh's equation and to the third power of the particle radius for DLS volume size. The DLS intensity-weighted sizes determined for each particle type were used to calculate the attachment efficiency and DLVO interaction energy profiles because these data are the least manipulated. It should be noted that the choice of particle size did not significantly affect the calculated attachment efficiency, calculations of the energy barrier to attachment discussed later, or the conclusion of this study as all three sizes are dominated by Brownian motion (Figures S7 and S8 in the SI).

The adsorbed mass of each organic coating was determined from TGA: 0.65, 8.4, and 4.2 wt % for citrate, GA, and PVP AgNPs, respectively (Figure S4 in the SI). Surface concentration in Table 1 was calculated from the adsorbed mass of each coating with the assumption that each AgNP is spherical and has a surface area in the range of 5−15 m^2/g, which is consistent with expectations for smooth spherical NPs with a primary particle diameter less than 30 nm.[24,25]

GA- and PVP-coated AgNPs have a relatively thick coating of high molecular weight polymer. As such, they are classified as "soft particles" and comprise an inner hard sphere of AgNPs covered with concentric layers of polymers. Conversely, citrate is a small organic acid molecule without any significant spatial extent and therefore a citrate AgNP is considered a hard sphere.

The surface potentials of GA- and PVP-coated AgNPs were significantly smaller than the ζ-potential of citrate AgNPs since their potentials are located at the boundary between the end of the adsorbed polymer layer and surrounding solution, rather than at the slip plane in the diffuse double layers as in Smoluchowski's model (Figure S9 in the SI). These small surface potentials of GA- and PVP-coated AgNPs imply that steric or electrosteric repulsions are the dominant repulsive interaction between the polymer-coated AgNPs and collector surfaces. In contrast to GA- and PVP-coated AgNPs, the repulsive interaction of citrate AgNPs with collector surfaces consists of only electrostatic repulsion derived from its high ζ-potential. The calculated ζ-potential of citrate AgNPs and surface potentials of PVP and GA AgNPs were used later to calculate DLVO interaction energy profiles for their attachment onto clean and OTS-coated glass beads.

Characterization of Collector Surfaces. The contact angle of water dropped on OTS-coated glass beads was 121° ± 7.5°, significantly higher than for glass beads that were not coated with OTS (33° ± 3.2°) (Figure S5 in the SI). It is important to note that surface roughness and heterogeneity may affect the absolute value of these measured contact angles, but the difference between the OTS-coated and uncoated glass beads is significant, indicating that the OTS-coated glass beads were indeed hydrophobic. The measured ζ-potentials of the clean and OTS glass beads at pH 8.1 were −48.64 ± 0.07 and −35.15 ± 0.36 mV, respectively. The decrease in the magnitude of charge for OTS-coated glass beads compared to uncoated ones also indicates OTS coverage of the glass beads. The difference of 13 mV between OTS-coated and uncoated glass beads is accounted for in the interaction energy calculated using DLVO.

Nanoparticle Transport through Clean and OTS-Coated Glass Beads. To investigate the role of hydrophobic surface on NP attachment, deposition experiments were conducted for the three AgNPs in columns containing varying amounts of clean and OTS-coated glass beads (Figure 1).

The attachment efficiency of the surface-modified AgNPs increased with increasing portions of hydrophobic OTS-coated glass beads in the column (Figure 1). In the cases of PVP- and GA-coated AgNPs, the attachment efficiency increased by a factor of approximately 4 and 2.5, respectively, as the portion of OTS-coated glass beads changes from 0% to 100%. The differences between the slopes of the lines for each AgNP types are statistically significant according to Student's *t*-tests on the pairs of AgNPs (see Student's *t* test in the SI). Attachment efficiencies are low overall due to the repulsive interactions between AgNPs and glass beads, both of which have a net negative surface potential.

The attachment efficiency $\alpha_{overall}$ of a polymer-coated nanoparticle in the presence of hydrophobic surfaces can be modeled by a linear combination of two surfaces in the column (clean glass beads and OTS-coated glass beads) using eq 3. A similar equation was used to describe attachment of colloids to "patchwise" heterogeneous media containing positively and negatively charged collectors.[26]

$$\alpha_{overall} = \theta\alpha_{hydrophobic\ surface} + (1-\theta)\alpha_{clean\ surface} \quad (3)$$

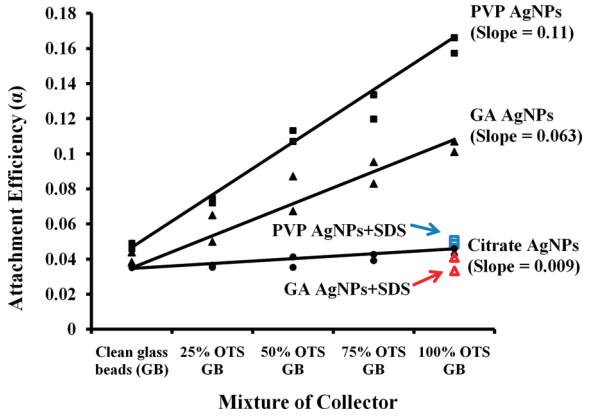

Figure 1. Attachment efficiency of three coated AgNPs as a function of the portion of OTS-coated (hydrophobic) surfaces in the column. The experimental attachment efficiencies (α_{exp}) were computed from eq 1. The single-collector contact efficiencies (η_0 = 0.024, 0.024, and 0.023 for GA, PVP, and citrate AgNPs, respectively) were calculated using eq 2 with the following parameter values: collector diameter = 350 μm, approach velocity = 2×10^{-4} m/s, Hamaker constant = 2.25×10^{-20} J, T = 298 K, Ag density = 1050 kg/m^3, water density = 1×10^3 kg/m^3, viscosity = 1×10^{-3} kg/ms, and porosity = 0.36. The trend lines were generated using a least-squares fit. The slopes of the lines are reported in parentheses. Attachment efficiency values calculated using the DLS volume-averaged and TEM sizes were not significantly different and are reported in the SI (Figure S7).

In eq 3, θ is the ratio of hydrophobic media to the total volume of media, and $\alpha_{hydrophobic\ surface}$ and $\alpha_{clean\ surface}$ represent the attachment efficiencies for the OTS-coated and clean glass surfaces, respectively. This model suggests that the overall attachment efficiency of a polymer-coated nanoparticle will be influenced by the fraction of hydrophobic surfaces in the environment. Moreover, the different slopes of the lines suggest that the type of surface coating will also affect the value of the overall attachment efficiency. However, in addition to making the glass bead surface hydrophobic, the OTS coating also reduced the overall charge on the glass beads.

Total Interaction Modeling for Attachment of AgNPs. The total interaction energy based on classical DLVO and steric interactions was calculated to support the conclusion that the observed differences in slope between coatings is indeed due to the different coating types rather than due to differences in electrostatic repulsions. In all cases the (polymer-coated) particle−collector interaction is calculated by assuming a sphere−plate interaction. The DLVO energy is defined as the sum of attractive van der Waals and repulsive electrical double layer interactions. The van der Waals interaction (V_{vdW}) is computed as[27,28]

$$V_{vdW} = -\frac{Aa_p}{6h\left(1+\frac{14h}{\lambda}\right)} \quad (4)$$

where A is the Hamaker constant of the interacting media (AgNP−water−soda lime glass beads), a_p is the intensity-weighted size of AgNPs measured by DLS, h is the distance between the nanoparticle and the collector, and λ is the characteristic wavelength of the dielectric (assumed to be 100 nm) . The Hamaker constant was calculated as

$$A = (A_{11}{}^{1/2} - A_{33}{}^{1/2})(A_{22}{}^{1/2} - A_{33}{}^{1/2}) \quad (5)$$

where $A_{11} = 3.85 \times 10^{-19}$ J for Ag,[29] $A_{22} = 6 \times 10^{-20}$ J for soda lime, and $A_{33} = 3.7 \times 10^{-20}$ J for water. The calculated Hamaker constant between AgNPs and glass beads in aqueous media is 2.25×10^{-20} J.

Electrical double layer interaction (V_{EDL}) is calculated using Eq 6[30]

$$E_{EDL} = \pi\varepsilon_0\varepsilon_r a_p \left\{ 2\varphi_c\varphi_p \ln\left[\frac{1+\exp(-\kappa h)}{1-\exp(-\kappa h)}\right] + (\varphi_c{}^2 + \varphi_p{}^2)\ln[1-\exp(-2\kappa h)]\right\} \quad (6)$$

where ε_0 is the dielectric permittivity in a vacuum, ε_r is the relative dielectric permittivity of water at 25 °C, κ is the inverse Debye length, and φ_c and φ_p are the ζ-potentials of the collectors and the electrokinetic potentials for three coated AgNPs.

With adsorbed polymer layers, such as GA and PVP, steric repulsion also needs to be considered. Steric interaction is defined as the sum of osmotic and elastic repulsive energies. Upon the approach of a spherical particle coated with a polymeric layer to a uncoated flat surface (we assume that OTS surface has no influential polymeric layer), osmotic and elastic repulsion energies are defined in the range of $0 < h \le d$,[31] where h is the distance between a particle and a flat surface, and d is the layer thickness. The osmotic energy (V_{osm}) is given as[31−33]

$$V_{osm} = \frac{2\pi a_p \Phi_p{}^2 N_A}{\overline{V}}\left(\frac{1}{2} - \chi\right)(d-h)^2 \quad (7)$$

where Φ_p is the volume fraction of the polymer, N_A is Avogadro's number, $\overline{V}$ is the molar volume of the water, χ is the Flory−Huggins solvency parameter (assumed to be 0.45 for PVP, 0.47 for GA).[34] The volume fraction of adsorbed polymer was estimated as

$$\Phi_p = 3\frac{\Gamma_{max} a_p{}^2}{\rho_p[(d+a_p)^3 - a_p{}^3]} \quad (8)$$

where ρ_p is the polymer density, which is set to be 1.29 and 1.35 g/cm^3 for PVP and GA, respectively, and Γ_{max} is the maximum surface concentration. The calculated Φ_p values for PVP and GA are 0.48 and 0.08, respectively.

The elastic repulsion energy (V_{elas}) is calculated using eq 9[32,35]

$$V_{elas} = \frac{2\pi a_p N_A \Phi_p d^2 \rho_p}{M_w}\left[\frac{2}{3} - \frac{1}{6}\left(\frac{h}{d}\right)^3 - \left(\frac{h}{2d}\right) + \left(\frac{h}{d}\right)\ln\left(\frac{h}{d}\right)\right] \quad (9)$$

where M_w is molecular weight of the polymer.

Total Interaction Profiles To Interpret Attachment of Nanoparticles. Figure 2 shows the total interaction energy profiles for citrate AgNPs ($V_{tot} = V_{vdW} + V_{EDL}$) as well as GA- and PVP-coated AgNPs ($V_{tot} = V_{vdW} + V_{EDL} + V_{osm} + V_{elas}$) computed from eqs 4−9. It is worth mentioning that all the interactions were assumed to be linear and additive in calculating the total interaction energy[36] as is conventionally done, although steric and electrostatic repulsions are not completely independent.[34]

The DLVO interaction energy profiles indicated substantial repulsive energy barriers to (Φ_{max}) the primary minimum for both clean and 100% OTS glass beads: $53k_BT$ and $31k_BT$ for citrate AgNPs, $918k_BT$ and $904k_BT$ for GA AgNPs, $714k_BT$ and $700k_BT$ for PVP AgNPs, respectively, and are significantly greater than the thermal energy at 23 °C ($\sim 0.5k_BT$). Nanoparticles may deposit in the secondary energy minimum ($\Phi_{2°min}$); however,

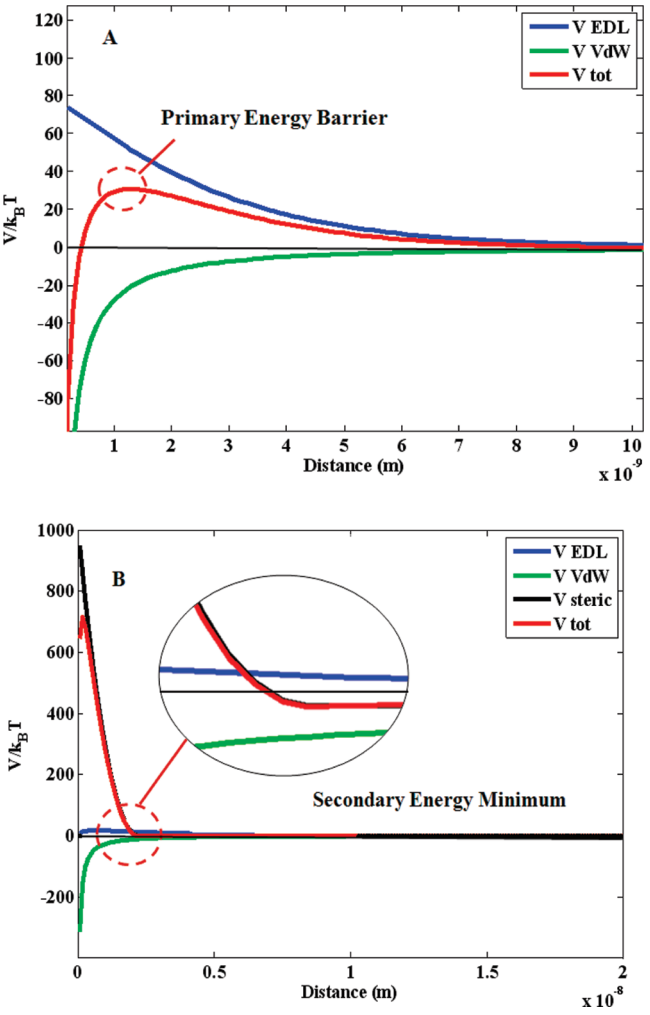

Figure 2. Total interaction energy profiles between AgNPs and OTS-coated glass beads: citrate AgNPs (top) and PVP AgNPs (bottom). The interaction profile for GA AgNPs is similar to that of PVP AgNPs and is not shown for clarity. DLVO interaction energy profiles calculated using the DLS volume-averaged size and TEM size give similar results and identical trends (Figure S8 in the SI).

due to the shallow secondary minima for clean and 100% OTS glass beads ($-0.5k_BT$ and $-0.6k_BT$ for citrate AgNPs, $-0.6k_BT$ and $-0.6k_BT$ for GA AgNPs, $-0.9k_BT$ and $-1.0k_BT$ for PVP AgNPs), particles are unlikely to attach to collector surfaces, which is consistent with the low attachment efficiencies of the AgNPs on the clean glass beads, as shown in Figure 1.

The total energy profiles based on DLVO and steric interactions, as is commonly used to model attachment of coated NPs to surfaces, indicate that the effect of hydrophobicity of the glass beads on attachment efficiencies of GA and PVP AgNPs should be similar to that of citrate AgNPs because the differences among the secondary energy minima of GA, PVP, and citrate AgNPs are trivial. This was not the case (Figure 1). One reason for the observed increase in deposition of GA and PVP AgNPs onto OTS-coated glass beads compared to citrate AgNPs is the hydrophobic attraction between the coatings of the AgNPs and the OTS surface. To test this hypothesis, the relative degree of hydrophobicity of the organic coatings was measured from their solubility; it is known that the aqueous solubility of a polymer increases as the hydrophobicity

of the polymer decreases. In addition, the relative hydrophobicity of AgNPs with different coatings were measured on the basis of partitioning of a hydrophobic dye between NP surfaces and water.

Hydrophobicity of AgNPs and Organic Coatings. To obtain the relative solubility among the organic coatings, we added ammonium sulfate (salt) into organic coating in buffer solution as previously described and measured the salt concentration at which polymer begins to precipitate (Figure 3A). As ammonium sulfate was added to each of organic coating solution, PVP precipitates at the lowest ammonium sulfate concentration, followed by GA and then citrate. This indicates that the most hydrophobic coating is PVP, followed by GA and then citrate. This is consistent with the chemical structures of each coating. PVP is uncharged with an amide group that favors dissolution. However, the polymer backbone has significant hydrophobic moieties (six carbons per monomer unit) that are hydrophobic, resulting in precipitation as the salt concentration increases. Gum arabic generally consists of high molecular weight polymers of polysaccharides (90%) and glycoprotein (10%) that are more hydrophilic than PVP. Citrate is a small molecular weight carboxylic acid that is very hydrophilic and miscible in water.

The relative hydrophobicity of the coated AgNPs rather than just the coating was also measured (Figure 3B). The slope of the curves in Figure 3B represents the linear adsorption coefficient for Rose Bengal (RB), a hydrophobic dye, onto the AgNPs (eq 10). These values were calculated to be 0.009 for PVP AgNPs, 0.007 for GA AgNPs, and 0.001 for citrate AgNPs and are statistically significant based on a Student's *t* test to each pair of AgNPs; *p*-values are 0.004 for PVP vs GA AgNPs and less than 0.001 for GA vs citrate AgNPs, and PVP vs citrate AgNPs.

$$\text{slope} = \frac{\dfrac{\text{mg of RB on NP}}{\text{mg of RB in water}}}{\dfrac{\text{mg of NP}}{\text{L of water}}} = \frac{C_{\text{RB(s)}}}{C_{\text{RB(w)}}} = K_{\text{RB}}\ (\text{L/mg NP}) \tag{10}$$

A greater slope indicates greater particle hydrophobicity, meaning that hydrophobicity of the PVP AgNPs was greatest, followed by GA AgNPs and the citrate AgNPs. This is consistent with measurements of the coatings alone and suggests that the surface hydrophobicity of AgNPs largely depends on the hydrophobicity of organic coatings.

The sensitivity of the coated AgNPs to increasing amounts of hydrophobic surface (OTS-coated glass) followed the order of hydrophobicity of organic coatings; it was greatest for the most hydrophobic PVP, followed by GA and then citrate. Nonpolar organic materials with low aqueous solubility can have strong attractions to hydrophobic surfaces in aqueous environments through hydrophobic interaction.[15,37,38] Hydrophobic interaction is a consequence of the arrangement of water molecules in the vicinity of hydrophobic surfaces. When AgNPs coated with a hydrophobic polymer approach the hydrophobic (OTS-coated) surfaces, water molecules in contact with hydrophobic moieties tend to be displaced into the bulk solution to reduce the total free energy of the system, leading to favorable interaction between hydrophobic moieties, the polymer coating, and the hydrophobic OTS-coated surface.[39,40] Despite many studies on hydrophobic interactions, a general quantitative expression for the magnitude of hydrophobic attraction in aqueous solution remains elusive.[15] Even though the hydrophobic attraction energy cannot be calculated, the fact that deposition onto hydrophobic surfaces increased

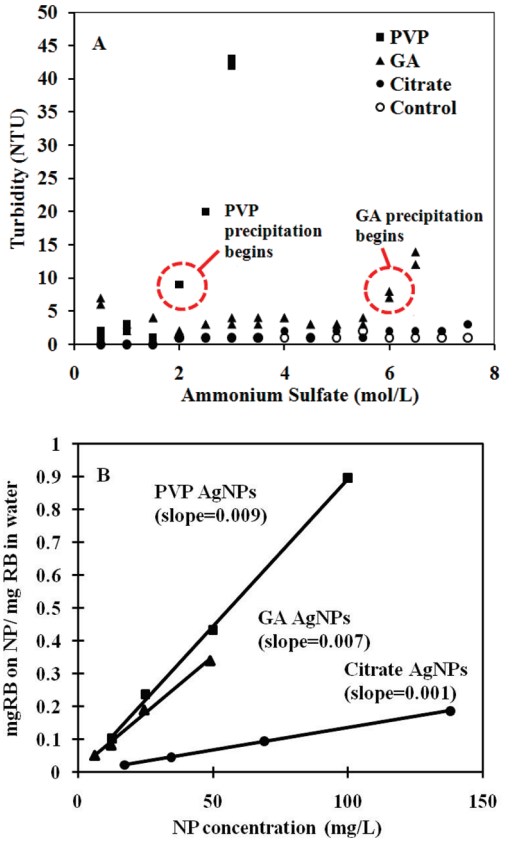

Figure 3. (A) Relative hydrophobicity of organic coatings alone determined using the "cloud point" precipitation method. (B) Relative hydrophobicity of surface-coated AgNPs determined by measuring partitioning of the hydrophobic dye Rose Bengal between AgNP surfaces and water.

with increasing hydrophobicity of the AgNPs suggests that hydrophobic interactions are responsible for the higher attachment of PVP and GA AgNPs onto OTS-covered surfaces compared to citrate AgNPs.

To further confirm the influence of hydrophobic interaction on the attachment of the surface-coated AgNPs, a second series of column experiment was performed as described in the method section. SDS, an anionic surfactant, adsorbs onto and masks hydrophobic surfaces of OTS glass beads, preventing hydrophobic interaction between the AgNPs and the OTS glass beads. In these columns, the attachment efficiencies of PVP and GA AgNPs were reduced to be close to the attachment efficiency of citrate AgNPs (Figure 1), indicating that the hydrophobic interaction between the AgNPs and the hydrophobic surfaces indeed controls deposition in the columns. It should be noted that the addition of SDS is known to have little impact on the surface charge of glass beads.[41,42]

■ ASSOCIATED CONTENT

Supporting Information. Surface-modified AgNPs Synthesis; Figures S1 and S2 show the NP size distributions as observed by DLS and TEM, respectively; Ohshima's soft particle analysis to estimate adsorbed layer properties on nanoparticles; Figure S3 shows the electrophoretic mobility of the three coated NPs as a function of ionic solution concentration; Figure S4 shows the TGA results for AgNPs and organic coatings; Figure

S5 shows the relative hydrophobicity of OTS-covered glass beads; Figure S6 shows the breakthrough curves generated from column experiments; Figure S7 shows attachment efficiency of each coated AgNP calculated using DLS volume-averaged size and TEM size; Figure S8 shows DLVO interaction energy profiles for citrate and PVP AgNPs based on TEM size; Figure S9 shows schematic images for the ζ-potential in Smoluchowski's model and the surface potential in Ohshima's model; Student's *t* test to compare linear regression. This material is available free of charge via the Internet at http://pubs.acs.org.

AUTHOR INFORMATION

Corresponding Author

*E-mail: glowry@cmu.edu; tel: 412-268-2948; fax: 412-268-7813.

ACKNOWLEDGMENT

This research was funded by the NSF Center for Environmental Implications of Nanotechnology (EF-0830093). The authors thank Ms. Stacey Louie for her Matlab code for Ohshima's analysis.

REFERENCES

(1) Elimelech, M., Gregory, J, Jia, X, Williams, R *Particle Deposition and Aggregation*, 1st ed.; Butterworth-Heinemann: Woburn, MA, 1995.

(2) Tufenkji, N. Modeling microbial transport in porous media: Traditional approaches and recent developments. *Adv. Water Resour.* **2007**, *30*, 1455–1469.

(3) Hermansson, M. The DLVO theory in microbial adhesion. *Colloids Surf. B* **1999**, *14*, 105–119.

(4) Jin, Y.; Flury, M. Fate and transport of viruses in porous media. *Adv. Agron.* **2002**, *77*, 39–102.

(5) Van Oss, C. J. *Interfacial Forces in Aqueous Media*; M. Dekker: New York, 1994.

(6) Absolom, D. R.; Lamberti, F. V.; Policova, Z.; Zingg, W.; Vanoss, C. J.; Neumann, A. W. Surface thermodynamics of bacterial adhesion. *Appl. Environ. Microb.* **1983**, *46*, 90–97.

(7) Vanloosdrecht, M. C. M.; Lyklema, J.; Norde, W.; Schraa, G.; Zehnder, A. J. B. The role of bacterial-cell wall hydrophobicity in adhesion. *Appl. Environ. Microb.* **1987**, *53*, 1893–1897.

(8) Lecoanet, H. F.; Bottero, J. Y.; Wiesner, M. R. Laboratory assessment of the mobility of nanomaterials in porous media. *Environ. Sci. Technol.* **2004**, *38*, 5164–5169.

(9) Wiesner, M. R.; Lowry, G. V.; Jones, K. L.; Hochella, M. F.; Di Giulio, R. T.; Casman, E.; Bernhardt, E. S. Decreasing uncertainties in assessing environmental exposure, risk, and ecological implications of nanomaterials. *Environ. Sci. Technol.* **2009**, *43*, 6458–6462.

(10) Mayya, K. S.; Schoeler, B.; Caruso, F. Preparation and organization of nanoscale polyelectrolyte-coated gold nanoparticles. *Adv. Funct. Mater.* **2003**, *13*, 183–188.

(11) Liu, J. F.; Zhao, Z. S.; Jiang, G. B. Coating Fe_3O_4 magnetic nanoparticles with humic acid for high efficient removal of heavy metals in water. *Environ. Sci. Technol.* **2008**, *42*, 6949–6954.

(12) Amirbahman, A.; Olson, T. M. Transport of humic matter-coated hematite in packed-beds. *Environ. Sci. Technol.* **1993**, *27*, 2807–2813.

(13) Phenrat, T.; Saleh, N.; Sirk, K.; Kim, H. J.; Tilton, R. D.; Lowry, G. V. Stabilization of aqueous nanoscale zerovalent iron dispersions by anionic polyelectrolytes: Adsorbed anionic polyelectrolyte layer properties and their effect on aggregation and sedimentation. *J. Nanopart. Res.* **2008**, *10*, 795–814.

(14) Phenrat, T.; Song, J. E.; Cisneros, C. M.; Schoenfelder, D. P.; Tilton, R. D.; Lowry, G. V. Estimating attachment of nano- and submicrometer-particles coated with organic macromolecules in porous media: Development of an empirical model. *Environ. Sci. Technol.* **2010**, *44*, 4531–4538.

(15) Meyer, E. E.; Rosenberg, K. J.; Israelachvili, J. Recent progress in understanding hydrophobic interactions. *Proc. Natl. Acad. Sci. U. S. A.* **2006**, *103*, 15739–15746.

(16) Kumar, N.; Garoff, S.; Tilton, R. D. Experimental observations on the scaling of adsorption isotherms for nonionic surfactants at a hydrophobic solid−water interface. *Langmuir* **2004**, *20*, 4446–4451.

(17) Shoults-Wilson, W. A.; Reinsch, B. C.; Tsyusko, O. V.; Bertsch, P. M.; Lowry, G. V.; Unrine, J. M. Effect of silver nanoparticle surface coating on bioaccumulation and reproductive toxicity in earthworms (*Eisenia fetida*). *Nanotoxicology* **2010**, 1–13.

(18) Ohshima, H. Electrophoresis of soft particles. *Adv. Colloid Interface* **1995**, *62*, 189–235.

(19) Bachmann, J.; Horton, R.; Van Der Ploeg, R. R.; Woche, S. Modified sessile drop method for assessing initial soil−water contact angle of sandy soil. *Soil. Sci. Soc. Am. J.* **2000**, *64*, 564–567.

(20) Tufenkji, N.; Elimelech, M. Correlation equation for predicting single-collector efficiency in physicochemical filtration in saturated porous media. *Environ. Sci. Technol.* **2004**, *38*, 529–536.

(21) Andrews, B. A.; Schmidt, A. S.; Asenjo, J. A. Correlation for the partition behavior of proteins in aqueous two-phase systems: Effect of surface hydrophobicity and charge. *Biotechnol. Bioeng.* **2005**, *90*, 380–390.

(22) Hjertén, S. *Hydrophobic Interaction Chromatography of Proteins, Nucleic Acids, Viruses, and Cells on Noncharged Amphiphilic Gels*; John Wiley & Sons, Inc.: New York, 2006.

(23) Muller, R. H. *Colloidal carriers for controlled drug delivery and targeting*; WVG/CRC Press: Stuttgart/Boca Raton, FL, 1991.

(24) Khanna, P. K.; Singh, N.; Kulkarni, D.; Deshmukh, S.; Charan, S.; Adhyapak, P. V. Water based simple synthesis of re-dispersible silver nano-particles. *Mater. Lett.* **2007**, *61*, 3366–3370.

(25) Wani, I. A.; Ganguly, A.; Ahmed, J.; Ahmad, T. Silver nanoparticles: Ultrasonic wave assisted synthesis, optical characterization and surface area studies. *Mater. Lett.* **2010**, *65*, 520–522.

(26) Elimelech, M.; Nagai, M.; Ko, C.-H.; Ryan, J. N. Relative insignificance of mineral grain zeta potential to colloid transport in geochemically heterogeneous porous media. *Environ. Sci. Technol.* **2000**, *34*, 2143−2148.

(27) Gregory, J. Approximate expressions for retarded vanderwaals interaction. *J. Colloid Interface Sci.* **1981**, *83*, 138–145.

(28) Elimelech, M.; Omelia, C. R. Effect of particle-size on collision efficiency in the deposition of Brownian particles with electrostatic energy barriers. *Langmuir* **1990**, *6*, 1153–1163.

(29) Butt, H. J.; Cappella, B.; Kappl, M. Force measurements with the atomic force microscope: Technique, interpretation and applications. *Surf. Sci. Rep.* **2005**, *59*, 1–152.

(30) Healy, T. W.; White, L. R. Ionizable surface group models of aqueous interfaces. *Adv. Colloid Interface* **1978**, *9*, 303–345.

(31) Amirbahman, A. Transport of humic matter-coated colloids in packed beds. Ph.D. Dissertation, University of California, Irvine, CA, 1994.

(32) Penrod, S. L.; Olson, T. M.; Grant, S. B. Deposition kinetics of two viruses in packed beds of quartz granular media. *Langmuir* **1996**, *12*, 5576–5587.

(33) Jucker, B. A.; Zehnder, A. J. B.; Harms, H. Quantification of polymer interactions in bacterial adhesion. *Environ. Sci. Technol.* **1998**, *32*, 2909–2915.

(34) Einarson, M. B.; Berg, J. C. Electrosteric stabilization of colloidal latex dispersions. *J. Colloid Interface Sci.* **1993**, *155*, 165–172.

(35) Evans, R.; Smitham, J. B.; Napper, D. H. Theoretical prediction of elastic contribution to steric stabilization. *Colloid Polym. Sci.* **1977**, *255*, 161–167.

(36) Kamiyama, Y.; Israelachvili, J. Effect of pH and salt on the adsorption and interactions of an amphoteric polyelectrolyte. *Macromolecules* **1992**, *25*, 5081–5088.

(37) Hummer, G.; Garde, S.; Garcia, A. E.; Pohorille, A.; Pratt, L. R. An information theory model of hydrophobic interactions. *Proc. Natl. Acad. Sci. U. S. A.* **1996**, *93*, 8951–8955.

(38) Lazaridis, T.; Paulaitis, M. E. Entropy of hydrophobic hydration—A new statistical mechanical formulation. *J. Phys. Chem.* **1992**, *96*, 3847–3855.

(39) Israelachvili, J. *Intermolecular and Surface Forces*; Academic Press: New York, 1991.

(40) Bishop, E. J.; Fowler, D. E.; Skluzacek, J. M.; Seibel, E.; Mallouk, T. E. Anionic homopolymers efficiently target zerovalent iron particles to hydrophobic contaminants in sand columns. *Environ. Sci. Technol.* **2010**, *44*, 9069–9074.

(41) Tufenkji, N.; Elimelech, M. Breakdown of colloid filtration theory: Role of the secondary energy minimum and surface charge heterogeneities. *Langmuir* **2005**, *21*, 841–852.

(42) Litton, G. M.; Olson, T. M. Colloid deposition kinetics with surface-active agents—Evidence for discrete surface-charge effects. *J. Colloid Interface Sci.* **1994**, *165*, 522–525.